Int. J. Electrochem. Sci., 15 **(2020)** 1942 – 1948, doi: 10.20964/2020.03.17

International Journal of
ELECTROCHEMICAL
SCIENCE
www.electrochemsci.org

Short Communication

One-pot Hydrothermal Synthesis of MoS_2 Porous Nanospheres and Their Electrochemical Properties

Hongdong Liu[1,#],Yu Lei[1,#], Ye Lin[1], Lei Zhang[2,] , Yao Lu[3,*]*

[1] College of Materials Science and Engineering, Chongqing University of Arts and Sciences, Chongqing 402160, PR China
[2] College of Life Science, Chongqing Normal University, Chongqing 401331, PR China
[3]College of Biological and Chemical Engineering, Guangxi University of Science and Technology, Liu zhou 545006, PR China
[#] Hongdong Liu and Yu Lei are co-first authors
[*]E-mail: leizhang0215@126.com (Lei Zhang), 41039639@QQ.com (Yao Lu)

Received: 14 October 2019 / *Accepted:* 16 December 2019 / *Published:* 10 February 2020

In this paper, we have sucessfully prepared MoS_2 porous nanospheres by one-step hydrothermal method and further applied to the anode materials for LIBs. MoS_2 porous nanospheres show high lithium storage property and good cycling performance. The discharge capacity and charge capacity of MoS_2 nanospheres are up to 439 mAh/g and 440 mAh/g, respectively, after 500 cycles at the current density of 1 A/g. Large specific surface area and porous structure of MoS_2 nanospheres can improve the reversible capacity and cycle stability of LIBs, and they will show great potential to replace graphite anode materials.

Keywords: MoS_2, nanospheres, anode materials, lithium ion batteries

1. INTRODUCTION

Currently, lithium ion batteries (LIBs) have become predominant battery technology, because of high energy density, light weight, long cycle life, and ecofriendly features [1, 2]. However, commercial LIBs can not meet the increasing capacity demand because of the low theoretical gravimetric capacity (372 mAh g^{-1}) of graphite anode materials[3, 4]. Thus, Efforts in developing new electrode materials with higher capacity and longer cycle life have step into an unprecedented level. Up to now, several distinguished candidates have been identified, for example metal sulfides[5-7], metal selenides[8, 9] and transition metal oxides[10-12]. Among them, molybdenum disulfide (MoS_2) as an anode material for LIBs has attracted considerable attention owing to its high theoretical capacity (1007 mAh/g) ,structure stability, and relatively low price. However, this material undergoes a

large volume expansion/contraction during charge/discharge process, which limits its further development. So far, several approaches have been applied to overcome this drawback of pure MoS_2 anode materials. The design and synthesis of various morphologies of MoS_2 samples has proven a good method for the improvement of Li-ion diffusion property and conductivity[13, 14]. Such as, Feng prepared MoS_2 hierarchical nanostructure by hydrothermal methord under the molar ration of S/Mo=4.3:1 at 200 ºC for 24h. As lithium ion battery anode material,the MoS_2 hierarchical nanostructure exhibit superior cycling sability at high current density[15]. Guo synthesised few layer MoS_2 nanosheets and these MoS_2 nanosheets exhibit the highest specific reversible capacity of 1097 mA h g^{-1} at a current density of 50 mA g^{-1}after 25 cycles[16]. According to previous studies[17-19], porous nanospheres have larger specific surface area, so they have better electrochemical lithium storage performance. Hence, MoS_2 porous nanospheres are prepared by one-step hydrothermal method and further applied to the anode materials for LIBs, and show high lithium storage property and good cycling performance.

2. EXPERIMENTAL SECTION

2.1 Synthesis of materials

In a typical synthesis process, 3 g of CH_4N_2S, 0.565 g of Na_2MoO_4 and 1 g of PVP were dissolved in 30 ml deionized. Then, the resulting mixed solution was transferred into a 40 ml PTFE-lined autoclave and kept at 180 ºC for 12 h. After that, taked out the reactor and cooled to room temperature. Lastly, the black precipitate was washed several times with deionized water and anhydrous ethanol, respectively, and dried in a drying oven.

2.2 Characterization

X-ray diffraction patterns were performed on a TD-3500 X-ray diffractometer equipped with Cu/Ka radiation (ë=0.15406 nm) at a scanning rate of 4º min^{-1} in the range of 10º-80º. The morphologies and microstructure of MoS_2 were investigated by field emission scanning electron microscopy (FESEM, Sigma 500). The specific surface area and pore structure were determined by nitrogen adsorption/desorption at 77 K (Micromeritics ASAP 2020).

2.3 Electrochemical tests

The electrochemical properties of MoS_2 nanospheres were obtained by CR2032-type coin cells test. The working electrodes of CR2032-type coin cells were comprised of 80 wt% MoS_2 nanospheres as active material, 10 wt% acetylene black as conductive additive, and 10 wt% PVDF as polymer binder. The pure lithium was used as reference electrode and counter electrode. the separator was Celgard 2400 microporous polypropylene. The electrolyte consisted of the mixture of 1 M $LiPF_6$ dissolved in ethylene carbonate (EC) and dimethyl carbonate (DMC) (1:1 v/v). The galvanostatic

charge-discharge measurements were implemented on a Battery Testing System (Neware BTS-610) between 0.01 and 3.0 V vs Li/Li^+ at the different current densities.

3. RESULTS AND DISCUSSION

The crystalline structures of the as-produced samples were presented in Fig. 1. The main three characteristic diffraction peaks at 8.9, 33, and 59.8° are associated with the (002), (100) and (110) planes of hexagonal MoS_2 (JCPDS No. 37-1492), which is similar to that reported in the previous literature[20]. Moveover, a slightly wider peak at 17.5 ° as well as a low sharp peak at 39 ° are observed and can be indexed to expanded (004) and (103) planes of MoS_2, respectively. All of the diffraction peaks are ascribed to the well-crystallized MoS_2 with a hexagonal phase.

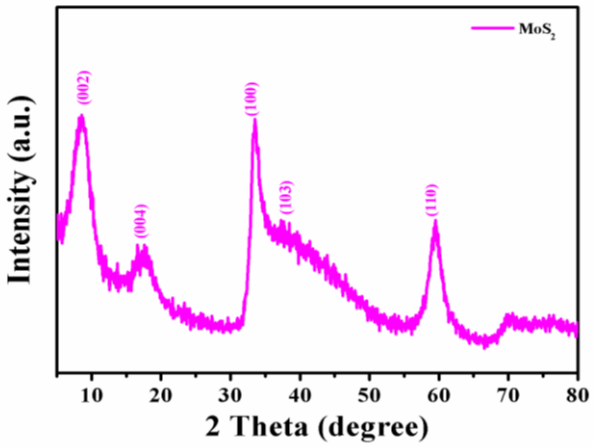

Figure 1. XRD patterns of MoS_2

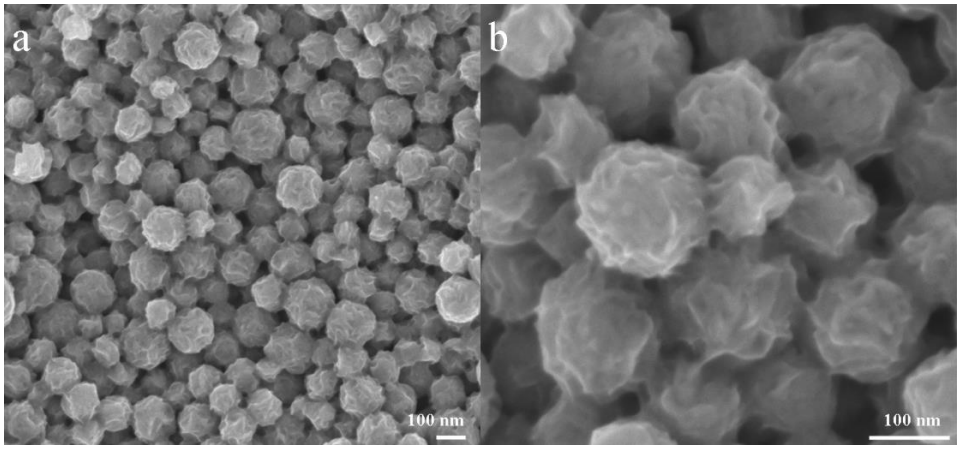

Figure 2. (a) and (b) FESEM images of MoS_2

The microstructure and morphology of the as-prepared MoS_2 were investigated by SEM. As shown in Fig. 2a and 2b, a large number of MoS_2 nanospheres are evenly distributed. The MoS_2 nanospheres perform a uniform size distribution from 50 to 120 nm. Fig. 2b clearly shows that MoS_2 nanospheres are composed of assembly nanosheets and the surface of the nanospheres is uneven,

which is beneficial to contact with the electrolyte of LIBs.

As shown in Fig.3, the specific surface area of MoS_2 nanospheres is 10.277 m^2/g, the pore volume of MoS_2 nanospheres is 0.066 cm^3/g. The nitrogen adsorption-desorption curve belongs to type IV isotherm with an average pore diameter of 30 nm. It is obvious that MoS_2 nanosphere is a mesoporous material. The adsorption curve of the isotherm is not consistent with the desorption curve. Obvious hysteresis loops can be observed, and the hysteresis loops belong to type H4. It is important that mesoporous materials are favorable for lithium ion storage.

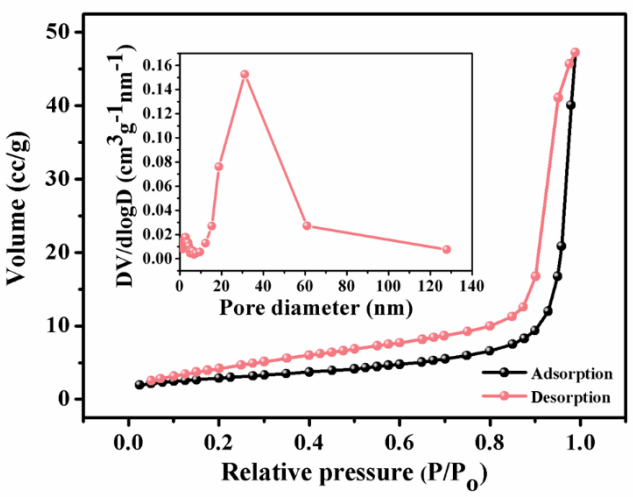

Figure 3. N_2 adsorption/desorption isotherms of MoS_2, inset of pore size distribution of MoS_2

As shown in Fig. 4 (a), the first discharge capacity of MoS_2 nanospheres is 1189 mAh/g, the first charge capacity is 842 mAh/g , and the first coulomb efficiency is 70.8%. The first discharge capacity is higher than the theoretical capacity of anode materials, and this phenomenon generally exists in oxides[21, 22], sulfides[23-25], selenides[26, 27] and other negative materials[28] of lithium-ion batteries. The main reason may be that during the first charging process, part of lithium ion is stored in the electrode material, part of lithium ion is adsorbed on the surface of the electrode material, and part of lithium ion is stored in the SEI film produced by the electrode material[29]. The first discharge capacity comes from the above three parts, so the first discharge capacity will be higher than the theoretical capacity. The third discharge capacity and charge capacity decrease to 765 mAh/g and 797 mAh/g, respectively. In the first three charging curves, there is a voltage platform between 2.1-2.4v, which is mainly due to the formation of SEI film[30]. At the current density of 0.1A/g, after 100 cycles, the discharge capacity and charging capacity of MoS_2 nanospheres are up to 535 mAh/g and 558 mAh/g, respectively, in Fig. 4 (b). The rate performance of MoS_2 microspheres is shown in Fig.4(c). After 60 cycles, the discharge capacity and charge capacity of MoS_2 nanospheres are 668 mAh/g and 673 mAh/g, respectively, at various current rates range from 0.1 to 1.5 A g^{-1}. As shown in Fig. 4 (c), MoS_2 nanospheres show better rate performance , especially at high current densities. In order to further test the cycling performance of MoS_2 nanospheres, the discharge capacity and charge capacity of MoS_2 nanospheres are up to 439 mAh/g and 440 mAh/g, respectively, after 500 cycles at the current density of 1A / g in Fig. 4 (d). Compared with the previously reported MoS_2 anode

materials from Table1, it shows that MoS_2 nanospheres have better electrochemical performance and they will show great potential to replace graphite anode materials. The reason for this better performance is mainly due to the porous structure of MoS_2 and its more uniform morphology.

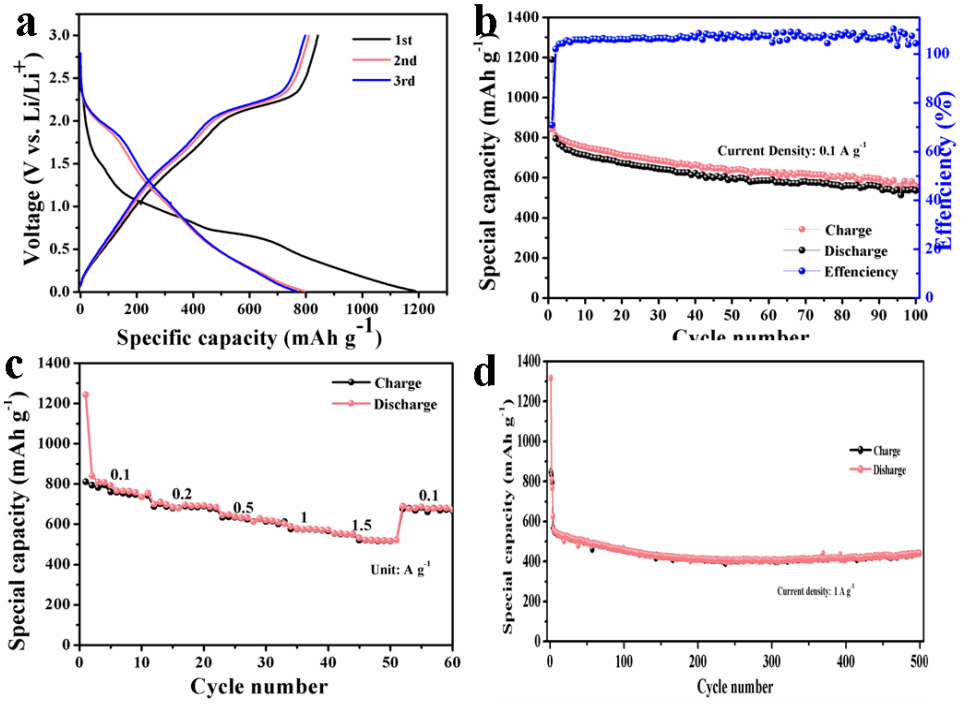

Figure 4. (a) Discharge/charge profiles at a current density of 0.1 A/g; (b)The electrochemical performances of MoS_2; (c) Rate performance of the samples at various current rates range from 0.1 to 1.5 A/g; and (d) Long-term cycling performance of the samples at a current density of 1 A/g for 500 cycles.

Table 1. Comparison of the electrochemical properties of MoS_2

Materials	Reversible capacity (mAh/g)	Cycle number (n)	Current density (mA/g)	References
MoS_2	391	30	400	[31]
MoS_2 nanostructure	478	50	100	[15]
MoS_2	479.1	100	100	[32]
Bulky MoS_2	about 100	100	200	[33]
TiO_2–MoS_2 hybrid	361.5	300	800	[34]
MoS_2/C nanocomposites	about 450	60	100	[35]
MoS_2 porous nanospheres	535	100	100	This work
	439	500	1000	

4. CONCLUSIONS

MoS_2 porous spheres were prepared by one-step hydrothermal method. And they are composed of assembly nanosheets. The size range of nanospheres is 50-120 nm. the specific surface area of MoS_2

nanospheres is 10.277 m^2/g, the pore volume of MoS_2 nanospheres is 0.066 cm^3/g. As the anode materials for LIBs, MoS_2 porous spheres show high lithium storage property and good cycling performance. They deliver high discharge /charge capacities of 1189/842 mAh/g at the current density of 0.1 A/g in the first cycling curves, after 100 cycles, the discharge capacity and charging capacity of MoS_2 nanospheres are up to 535 mAh/g and 558 mAh/g, respectively. Even at higher charge/discharge current density of 1 A/g, the discharge capacity and charge capacity of MoS_2 nanospheres are up to 439 mAh/g and 440 mAh/g, respectively. Large specific surface area and porous structure of MoS_2 nanospheres can improve the reversible capacity and cycle stability of LIBs.

ACKNOWLEDGEMENTS
This work is financially supported by the Technology and Basic and Frontier Research Program of Chongqing Municipality (cstc2018jcyjAX0701) and (cstc2017jcyjAX0326), and Major Program of Chongqing University of Arts and Sciences (P2017XC06), the Postgraduate Research Project Fund of Chongqing University of Arts and Sciences (M2017ME16).

References

1. H. Liu, S.-h. Luo, D.-b. Hu, X. Liu, Q. Wang, Z.-y. Wang, Y.-l. Wang, L.-j. Chang, Y.-g. Liu, T.-F. Yi, Y.-h. Zhang, A.-m. Hao, *Applied Surface Science*, 495 (2019) 143590.
2. F. Ghani, A. Raza, D. Kyung, H.-S. Kim, J. Lim, I.W. Nah, *Applied Surface Science*, 497 (2019) 143718.
3. H. Liu, Z. Hu, Y. Su, H. Ruan, R. Hu, L. Zhang, *Applied Surface Science*, 392 (2017) 777.
4. H. Liu, J. Huang, X. Li, J. Liu, Y. Zhang, K. Du, *Applied Surface Science*, 258 (2012) 4917.
5. C. Ding, D. Su, W. Ma, Y. Zhao, D. Yan, J. Li, H. Jin, *Applied Surface Science*, 403 (2017) 1.
6. H. Liu, L. Zhang, H. Ruan, *International Journal of Electrochemical Science*, 13 (2018) 4775.
7. K.-J. Huang, J.-Z. Zhang, Y. Liu, Y.-M. Liu, *International Journal of Hydrogen Energy*, 40 (2015) 10158.
8. X. Shang, S. Li, K. Wang, X. Teng, X. Wang, Q. Li, J. Pang, J. Xu, D. Cao, S. Li, *International Journal of Electrochemical Science*, 14 (2019) 6000.
9. H. Liu, Z. Li, L. Zhang, H. Ruan, R. Hu, *Nanoscale Research Letters*, 14 (2019) 237.
10. H. Liu, Z. Hu, Y. Su, R. Hu, L. Tian, L. Zhang, H. Ruan, *International Journal of Electrochemical Science*, 11 (2016) 8964.
11. Y. Yan, B. Wang, C. Yan, D.J. Kang, *Ceramics International*, 45 (2019) 15906.
12. M. Xiao, Y. Meng, C. Duan, F. Zhu, Y. Zhang, *Journal of Materials Science-Materials in Electronics*, 30 (2019) 6148.
13. L. Xu, L. Ma, T. Rujiralai, B. Liu, J. Zhang, W. Zhang, *Nanotechnology*, 30 (2019) 415402.
14. H. Li, Y. He, Q. Yang, J. Wang, S. Yan, J. Chen, *International Journal of Electrochemical Science*, 14 (2019) 8662.
15. H.J. Feng, W.J. Zheng, *Chemical Journal of Chinese Universities-Chinese*, 38 (2017) 1134.
16. C.P. Veeramalai, F. Li, H. Xu, T.W. Kim, T. Guo, *Rsc Advances*, 5 (2015) 57666.
17. W. Wei, P. Du, D. Liu, H. Wang, P. Liu, *Materials Letters*, 196 (2017) 191.
18. M. Sasidharan, N. Gunawardhana, C. Senthil, M. Yoshio, *Journal of Materials Chemistry A*, 2 (2014) 7337.
19. X. Kong, T. Mei, Z. Xing, N. Li, Z. Yuan, Y. Zhu, Y. Qian, *International Journal of Electrochemical Science*, 7 (2012) 5565.
20. B. Wang, Y. Xia, G. Wang, Y. Zhou, H. Wang, *Chemical Engineering Journal*, 309 (2017) 417.

21. L. Wang, J. Wu, Y. Chen, X. Wang, R. Zhou, S. Chen, Q. Guo, H. Hou, Y. Song, *Electrochimica Acta*, 186 (2015) 50.
22. H. Liu, J. Huang, X. Li, J. Liu, Y. Zhang, *Ceramics International*, 39 (2013) 3413.
23. H.D. Liu, L. Zhang, H.B. Ruan, *International Journal of Electrochemical Science*, 13 (2018) 4775.
24. J. He, Q. Li, Y. Chen, C. Xu, K. Zhou, X. Wang, W. Zhang, Y. Li, *Carbon*, 114 (2017) 111.
25. F.Z. Wang, F.G. Li, L. Ma, M.J. Zheng, *Chemistry-a European Journal*, 25 (2019) 14598.
26. P. Zhou, L.B. Chen, M.Y. Zhang, Q.Z. Huang, C. Cui, X. Li, L.P. Wang, L.W. Li, C. Yang, Y.H. Li, *Journal of Alloys and Compounds*, 797 (2019) 826.
27. Z.Y. Li, H.D. Liu, J.M. Huang, L. Zhang, *Ceramics International*, 45 (2019) 23765.
28. H. Liu, J. Huang, X. Li, J. Liu, Y. Zhang, *Journal of Wuhan University of Technology-Materials Science Edition*, 28 (2013) 220.
29. D. Wang, W. Zhou, Y. Zhang, Y. Wang, G. Wu, K. Yu, G. Wen, *Nanotechnology*, 27 (2016) 045405.
30. Y.H. Xu, C.C. Zhang, S.J. Kuang, K. Zhao, M. Chen, D.H. Xu, W.Y. Chen, X.Y. Yu, *Journal of Electroanalytical Chemistry*, 847 (2019) 113265.
31. X.F. Qian, Y.R. Wang, W. Zhou, L.P. Zhang, G.S. Song, S.Q. Cheng, *International Journal of Electrochemical Science*, 10 (2015) 3510.
32. Y. Liu, D.P. Tang, H.X. Zhong, Q.Y. Zhang, J.W. Yang, L.Z. Zhang, *Journal of Alloys and Compounds*, 729 (2017) 583.
33. S.C. Li, P. Liu, X.B. Huang, Y.G. Tang, H.Y. Wang, *Journal of Materials Chemistry A*, 7 (2019) 10988.
34. Y.J. Zhang, S.B. Zhao, X.Y. Zeng, J. Xiao, P. Dong, J.B. Zhao, S.G. Sun, L. Huang, X. Li, *Journal of Materials Science-Materials in Electronics*, 28 (2017) 9519.
35. X.Z. Guo, P.A. Yin, Z.C. Wang, H. Yang, *Journal of Sol-Gel Science and Technology*, 85 (2018) 140.